JOURNAL OF CATALYSIS 54, 372–383 (1978)

Steady-State Oxidation of Carbon Monoxide over Supported Noble Metals with Particular Reference to Platinum

NOEL W. CANT, P. C. HICKS, AND B. S. LENNON

School of Chemistry, Macquarie University, North Ryde, N.S.W. 2113, Australia

Received April 5, 1977; revised February 22, 1978

Activation energies, kinetic orders, and relative activities have been determined for the oxidation of CO by O_2 over five supported noble metals. With ruthenium drifts in reaction rate occurred for many hours following pressure and temperature changes but the initial responses were qualitatively similar to the simple behavior found for iridium, rhodium, and palladium (above 390 K), namely, kinetic orders near -1 and $+1$ in CO and O_2, respectively, and an activation energy near 100 kJ mol^{-1}. The platinum-catalyzed reaction had a much lower activation energy (56 kJ mol^{-1}), and the kinetic order was only slightly negative in CO with a possible tendency for these findings to change toward those found for the other metals at temperatures above 480 K. These results were compared with the predictions of a model which used parameters derived from measurements made under uhv conditions and/or with only one reactant present in the gas phase. The two reactions indicated were those oxygen molecularly adsorbed on a near complete carbon monoxide layer and between adsorbed oxygen atoms and gas-phase carbon monoxide molecules. The kinetic results which were common to each metal conformed to that expected for this latter reaction with the rate limited by CO desorption. Under these conditions the order of metal activity should be opposite to the order of heats of adsorption of carbon monoxide, and from the measurements available such a relationship did seem to hold.

INTRODUCTION

Over the past 10 years studies of the oxidation of carbon monoxide over platinum, a reaction first investigated by Langmuir (*1*) in 1922, have proceeded at several levels. At very low pressures, thermal desorption (*2–4*), low-energy electron diffraction (*5*), and molecular beam (*6*) techniques have been used to study the interaction of both gases with atomically clean ribbons and crystals and with preadsorbed layers on these surfaces. In consequence equations which describe adsorption, desorption, and reaction under these conditions are well developed (*6, 7*). In particular the molecular beam work of Pacia *et al.* (*6*) has provided rate constants for CO_2 production by Eley–Rideal and Langmuir–Hinshelwood reactions of adsorbed *atomic* oxygen. The existence of the former pathway has also been well established for palladium (*8–10*) and more recently for iridium (*11*).

The above schemes do not provide a ready way to remove complete carbon monoxide layers at temperatures below 400 K where carbon monoxide desorption becomes very slow. However, such removal does occur in the presence of a few Torr of oxygen when these metals are in supported form (*12, 13*), and in the case of Pt/SiO_2 a model involving reaction between a *molecularly* adsorbed oxygen and two adsorbed carbon monoxide molecules has been described (*12*).

0021-9517/78/0543-0372$02.00/0

Studies based on passage of simulated automobile exhaust gases over platinum in the form used for catalytic converters for pollution control form another class of studies (*14*). Since reaction under these conditions is exceedingly complex (*15*), it is necessary to resort to semi-empirical models (*14*) in explaining kinetic behavior. In consequence the correspondence between elementary steps under these conditions and those described earlier is unknown.

In the present work kinetic parameters and relative rates for the steady-state oxidation of carbon monoxide over five supported noble metals have been determined and compared with those expected by extrapolation of the uhv models to the conditions used. The only similar study using a catalyst with known surface area is that of McCarthy *et al.* (*16*) for CO oxidation in pure O_2 over 0.0035% Pt/α-Al_2O_3. They found it necessary to assume two reaction mechanisms in order to explain a transition from negative- to positive-order kinetics in carbon monoxide as the pressure of the latter was decreased below 300 N m^{-2}. Here we show that these findings are those expected by extrapolation of our model to their conditions but that quantitative agreement requires that the numerical value of one of the basic parameters, the reaction probability for the Eley–Rideal reaction referred to earlier, be much lower on small platinum particles than on the bulk metal.

METHODS

The supported metal catalysts were prepared by impregnation of the support by appropriate strength aqueous solutions of the corresponding metal salts, namely, $Ru(NO_3)_3$, $Pd(NO_3)_2$, and $Rh(NO_3)_3$ (Engelhard Industries) and H_2PtCl_6, $Pt(NH_3)_2(NO_2)_2$, $(NH_4)_2IrCl_6$, or H_2IrCl_6 (Alfa Inorganics). The supports were Cabosil HS5 silica (Cabot Corp.), γ-alumina (Harshaw Type 0104), and a standard silica–alumina (87% SiO_2, 13% Al_2O_3) cracking catalyst (Catoleum Pty Ltd). Following drying, each preparation was sieved to appropriate mesh sizes and reduced with a 10% hydrogen in helium gas stream at 350°C for 2 hr and then either evacuated or treated with flowing helium alone for a similar period at the same temperature. Metal surface areas were determined by the standard gas chemisorption methods outlined by Sinfelt and Yates (*17*).

Reaction rates were measured in a single-pass flow reactor operating near atmosphere pressure under essentially differential flow conditions (conversion, <10% in the minor reactant). The gas stream contained 0.1 to 10% each of carbon monoxide and oxygen, the balance being helium with a total flow rate in the range 0.5 to 4 cm^3/s as determined with a soap-bubble flow meter. Usual test conditions employed 40 to 1000 mg of 100- to 120-mesh catalyst contained in small Pyrex reactors, and tests with coarser mesh samples showed no evidence that the reaction was diffusion-limited. The gases used were standard commercial cylinder grade. Passage of the feed stream through cooled silica gel columns to remove water and similarly condensable contaminants had no effect on the measured rate, and this step was generally omitted once it was established that carbonyls were absent (see Results). Rate measurements were commenced after the catalysts had first been allowed to equilibrate with the reactant stream under reaction conditions for 16 hr. Subsequently data were gathered after allowing adequate time (usually 30 min) for rate stabilization following each change in experimental conditions. Rates (in moles of CO_2 per second per gram of catalyst) were calculated from measurements of the total flow rate and composition of the gas stream leaving the reactor. Metal activities under standard conditions were compared as turnover numbers defined as molecules (CO_2) per surface metal atom per second and calculated from the corresponding rates knowing the metal surface area and the average area occupied by a single metal atom.

The analysis system was a dual column gas chromatograph with thermistor-type detectors (Carle Inst.). Both columns were packed with 80- to 100-mesh Porapak Q–S, one maintained at 200 K for analysis of CO, O_2, and N_2 (if present) and the other at 273 K for CO_2 analysis. The CO_2 content could be reliably measured at concentrations of 50 ppm in a 10-cm^3 loop. Initially calibration was carried out periodically using a gas mixture of known composition, but in later work helium containing 0.5% neon was used as the carrier for the reactant stream thus providing an internal standard for every separation on the 200 K column.

RESULTS

Following a standard pretreatment the catalysts were cooled in a flow of helium to a suitable temperature and then contacted with the reactant stream. Frequently very high conversions were observed during the initial minutes of contact following which rates declined steadily over a period of hours to a constant value which was then maintained for a period of 1 week or more. Measurements of reaction orders and activation energies were made only with catalysts which had been on stream for at least 16 hr and, within a range of experimental conditions, were found to be quite reproducible. This was despite the fact that the actual activity in the lined-out state, when measured with a standard set of conditions, was found to vary by a factor of up to ±2, with palladium showing the most variation and rhodium the least. It proved impossible to isolate all factors which contributed to the variation, but certainly the actual values for the CO/O_2 ratio and the temperature at the time of initial contact contributed heavily. It was as though initial interaction formed a layer which blocked part of the surface and could not be removed by operation at the relatively low reaction temperatures being employed.

Pressure Dependences

The variation in reaction rate with the pressure of each reactant was determined

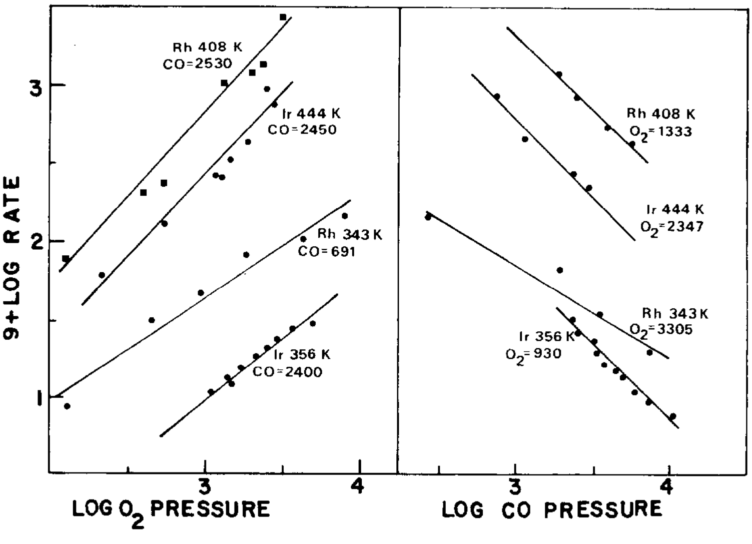

FIG. 1. Effect of CO and O_2 pressures on reaction rate over 5% Rh/SiO_2 and 5% Ir/SiO_2. Rates are in moles of CO_2 per gram of catalyst per second, pressures in newtons per square meter, and temperatures in degrees Kelvin.

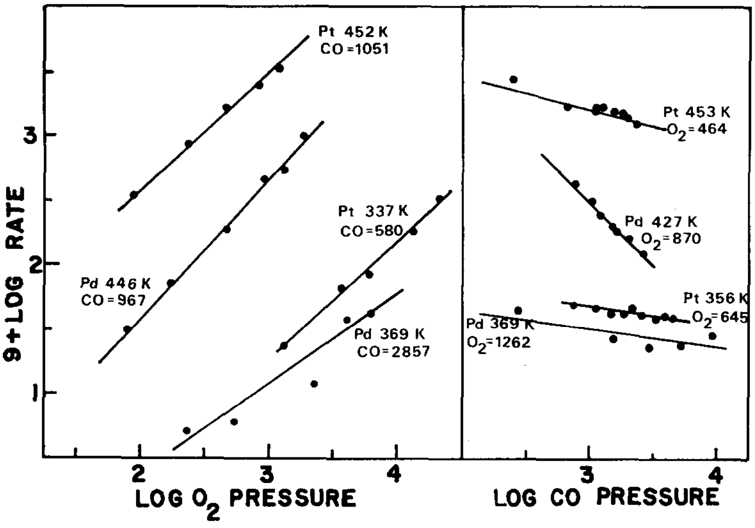

FIG. 2. Effect of CO and O_2 pressures on reaction rate over 5% Pd/SiO_2 and 5% Pt/SiO_2. Rates are in moles of CO_2 per gram of catalyst per second, pressures in newtons per square meter, and temperatures in degrees Kelvin.

at several temperatures, for various fixed pressures of the other reactant and for several samples of each supported metal. Some of the results for the 5% Rh, Pd, Ir, and Pt on silica catalysts are shown in Figs. 1 and 2 in the form of log–log plots (which are required to cover the wide range of pressures used). Kinetic orders, as calculated from the slopes of these and other similar graphs, are collected in Table 1, the indicated errors being sufficient to cover the range of values obtained.

TABLE 1

Activation Energies and Reaction Orders

Catalyst	Activation energy[a] (kJ mol^{-1})	Reaction order in CO	Reaction order in O_2
5% Ru/SiO_2	94 ± 17	−0.15 ± 0.2	0.4 ± 0.2
5% Rh/SiO_2	103 ± 5	−0.8 ± 0.2	0.9 ± 0.3
5% Pd/SiO_2	103 ± 10[b]	−0.8 ± 0.2[c]	0.9 ± 0.2
5% Ir/SiO_2	105 ± 6	−0.8 ± 0.1	1.0 ± 0.3
5% Pt/SiO_2	56 ± 6[d]	−0.2 ± 0.2[e]	0.9 ± 0.1

[a] With CO and O_2 pressures of 1300 and 650 N m^{-2}, respectively.

[b] Decreasing in values below 380 K.

[c] Less negative below 390 K.

[d] Increasing in value above 450 K.

[e] Tending more negative above 450 K.

With Rh, Ir, and Pd (above 390 K) the reaction was clearly first order in O_2 and close to inverse first order in CO. With Pt, however, the order in CO was only slightly negative. With this metal measurements at

TABLE 2

Time Dependence of Rate Following Changes in Oxygen Pressure Over Ru/SiO_2 at 351 K

Oxygen pressure (N m^{-2})	Elapsed time[a] (hr)	Rate[b] (× 10^9) (mol g^{-1} s^{-1})
1700	16.0	56.2
4000	0.1	95.0
4000	0.42	71.0
4000	0.9	59.9
4000	1.75	52.5
4000	2.85	47.0
4000	3.8	44.2
4000	5.3	38.2
4000	6.7	35.0
4000	7.7	34.1
1630	0.1	19.8
1630	0.25	20.7
1630	1.1	23.5
1630	22.5	37.3

[a] From change in oxygen pressure.

[b] With CO pressure constant at 920 N m^{-2}.

higher temperatures always showed a slightly more negative order in CO than lower temperature ones, but the difference was not much larger than the possible experimental error.

With all the above metals the rate responded virtually instantaneously to changes in pressure. Such was not the case with Ru/SiO$_2$ as may be seen from the data presented in Table 2. The *initial* response to a change in oxygen pressure was such as to indicate the same positive-order dependence operative with the other systems, but subsequent to the initial change the rate slowly relaxed in the opposite direction. Similarly with carbon monoxide the *initial* response was such as to indicate a negative reaction order following which the rate moved slowly back toward the initial value. One is tempted to conclude that part of the surface is covered by an inactive oxide layer, the amount of which is dependent on the CO/O$_2$ ratio. The results shown in Fig. 3 correspond to measurements made at a fixed time interval (1 hr) following each pressure change. It is recognized that the relationship presented, and the corresponding apparent kinetic orders presented in the first line of Table 1,

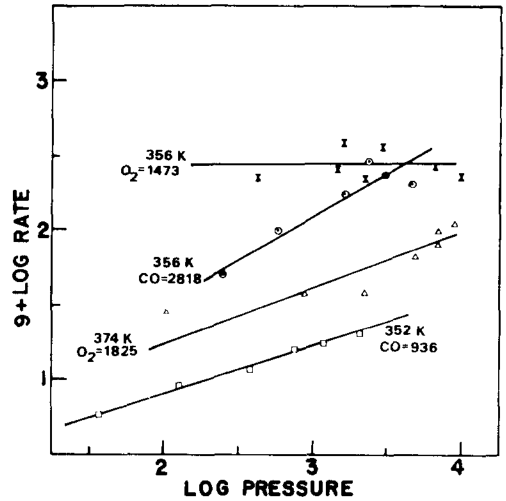

FIG. 3. Effect of CO and O$_2$ pressures on reaction rate over 5% Ru/SiO$_2$. Rates are in moles of CO$_2$ per gram of catalyst per second, pressures in newtons per square meter, and temperatures in degrees Kelvin. (The surface area of the ruthenium in the catalyst used at 356 K was higher than those used at the other temperatures.)

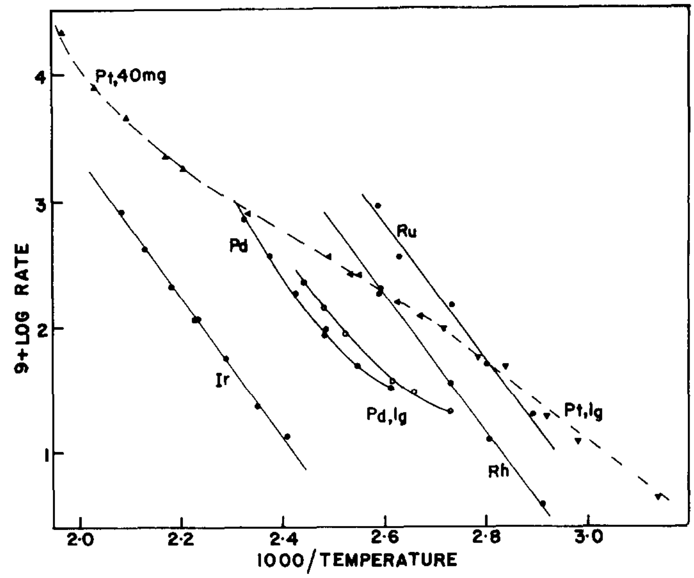

FIG. 4. Arrhenius plots for reaction over 5% metal on silica catalysts. Rates are in moles of CO$_2$ per gram of catalyst per second, corrected to CO and O$_2$ pressures of 1300 and 650 N m^{-2}, respectively. Catalyst weights were approx. 100 mg except as indicated.

TABLE 3

Effect of Particle Size and Support for Reaction over Iridium Catalysts

Catalyst	Dispersion	Activation energy[a]	Turnover number[b] ($\times 10^3$)	
			Surface atoms	Total atoms
5% Ir/SiO_2	0.04[c]	98 ± 3	90	4
5% Ir/SiO_2	0.12	106 ± 4	36	4
5% Ir/SiO_2	0.48	112 ± 6	29	14
5% Ir/SiO_2	0.38	97 ± 6	8	3
0.3% Ir/SiO_2	1.0	94 ± 2	4	4
0.3% Ir/Al_2O_3	0.28	107 ± 8	6	2
0.3% Ir/SiO_2-Al_2O_3	0.42	111 ± 4	5	2

[a] In kilojoules per mole with standard deviations as shown.

[b] In molecules (CO_2) per Ir atom per second measured at 450 K with CO and O_2 pressures of 1300 and 650 N m^{-2}, respectively (estimated error in measurement ± factor of 2).

[c] Produced by 1000 K calcination of the 5% Ir/SiO_2 sample with dispersion of 0.12.

do not refer to a steady state on the ruthenium surface.

Activation Energies

The effect of temperature on the reaction rate over each of the 5% silica-supported metals is shown in Fig. 4. These experiments were made with a close-to-stoichiometric ratio of CO and O_2, and the pressure dependences of Table 1 have been used to correct the data to actual pressures of 1300 and 650 N m^{-2}, respectively. In order to obtain the very wide range of rates shown for Pt/SiO_2, it was necessary to use several different weights of catalyst, as indicated. Over the greater part of the three orders of magnitude span in rates, these data conformed to a reasonably straight line, the slope of which was much less than that apparent for all the other metals (with the possible exception of palladium at the lowest temperature). At the highest temperature the slope for platinum did show an increase toward that found for the other metals, but the extent of this change was difficult to ascertain since rates now approached the maximum at which the differential reactor model could be maintained with even very small weights of our highly metal-loaded catalysts.

Activation energies calculated from a large number of plots of the type given in Fig. 4 are summarized in Table 1. Within experimental error reaction over Rh, Ir, Ru, and Pd showed the same apparent activation energy of about 100 kJ mol^{-1}. The value for Pt was much less except if calculated for the few highest temperature points.

Particle-Size and Support Effects

The effect of changes in metal particle size and support was investigated for iridium since this metal along with rhodium exhibited the simplest set of temperature and pressure dependences. The results are given in Table 3. Within likely experimental error the activation energy was the same for each catalyst. By contrast the turnover numbers varied by a factor of 20 and indeed showed rather less spread if the calculation was based on total metal atoms rather than estimated surface atoms. At least some of the spread may be due to experimental reasons in that measurement of iridium surface areas by hydrogen chemisorption has not been validated to the same extent as for platinum catalysts, especially in respect of possible hydrogen spillover. Furthermore even though pretreatment conformed to that used by Sinfelt and Yates (*17*) measurements by Escard *et al.* (*18*) suggest that complete reduction may necessitate rather more stringent conditions. Nevertheless the apparent lower activity of the better dispersed samples is in line with the findings of McCarthy *et al.* (*16*) for CO oxidation over Pt/α-Al_2O_3, and in addition Tauster and Murrell (*19*) noted a considerable difference between iridium catalysts of different metal loadings in respect of partitioning of CO between the CO + O_2 and CO + NO reactions.

Relative Activity

For three reasons it is difficult to make valid comparisons of the activity of noble

TABLE 4

Comparison of Activity of Noble Metals for Reactions of Carbon Monoxide and Oxygen

Metal	Turnover number (molecules per surface atom per second)					Heat of adsorption of carbon monoxide (kJ mol^{-1})[e]
	CO/H_2[a] at 540 K	C_2H_4/O_2[b] at 403 K	CO/O_2[c] at 400 K	CO/O_2[c] at 450 K	Calculated[d] for CO/O_2 at 450 K	
Ru	0.181	0.00016	0.07	1.63	0.022	121
Rh	0.013	0.000016	0.0065	0.25	—	—
Pd	0.012	0.032	0.001	0.031	0.000082	142
Ir	0.0018	0.0016	0.0001	0.0034	0.000027	146
Pt	0.0027	0.020	0.008	0.04	0.0072	125

[a] Reference (*20*) for alumina-supported materials.

[b] Calculated from Ref. (*21*) for silica-supported metals.

[c] This work for 5% metal on silica catalysts corrected to CO and O_2 pressures of 1300 and 650 N m^{-2}, respectively (estimated error ± factor of 2).

[d] See text.

[e] For hexagonally close-packed planes [Ref. (*7*)].

metals for carbon monoxide oxidation. In the first place the activity order will depend on the conditions chosen for comparison, since activation energies and pressure dependences are not identical. Second, as pointed out before, the steady-state activity varied with the conditions used to achieve that state. Third, the results of Table 3 show that uncontrolled factors influencing calculated turnover numbers were operative with one metal at least. These factors all contribute to the rather large range of error evident in the data given in Table 4 for relative activity at 400 and 450 K. Overall it is possible to say little more than that ruthenium is the most active and iridium the least active under these conditions.

For comparison purposes turnover data for two other systems, one involving CO the other O_2, are also given. It is apparent that the present results parallel the CO/H_2 reaction (*20*) much more closely than the C_2H_4/O_2 one (*21*).

Effect of Nickel on the Activity of Platinum

The discovery in the initial stages of the work that the steady-state activity of catalyst was dependent on its prior history led to a careful search for possible causes including a detailed analysis of used and as-prepared samples. The only detectable difference was a significantly greater amount of nickel in a few samples. The origin was nickel carbonyl present not as an impurity in the CO, but rather formed by room-temperature reaction between high-pressure CO and nickel plating within one of the pressure regulators and/or stainless-steel fittings. Contamination was eliminated when such pieces were replaced by copper and brass, and it should be stressed here that all of the results presented earlier were obtained subsequent to this change.

The effect that added nickel might have was briefly investigated for platinum, and the results of Table 5 were obtained. The turnover number for nickel was lower than that of platinum by several orders of magnitude, while the effect of adding nickel to platinum either by impregnation or by inadvertent introduction via nickel carbonyl was minimal. Nonetheless it would seem to be good practice to analyze used catalysts for nickel in all work using CO in a flow system especially as Ludlum and Eischens

TABLE 5

Effect of Nickel on Activity of Platinum

Weight percentage		Metal dispersion	Activation energy (kJ mol^{-1})	Turnover number at 400 K[a]
Platinum	Nickel			
5.0	<0.003	0.22	57 ± 4	0.013
5.0	0.42[b]	0.19	64 ± 3	0.013
4.5	0.5[c]	0.17	46 ± 4	0.025
nil	5.0	0.05	97 ± 3	0.00004

[a] In molecules of CO_2 per surface atom per second, calculated for CO and O_2 pressures of 1300 and 650 $N\ m^{-2}$, respectively.

[b] Introduced by decomposition of nickel carbonyl (see text).

[c] Introduced by coimpregnation.

(*22*) also reported contamination by carbonyls formed by CO reacting with heated stainless steel.

DISCUSSION

Our results indicate that the activation energy and pressure dependences for the oxidation of carbon monoxide over platinum are different from those prevailing with the other four metals. Thus for palladium we find an activation energy near 100 kJ mol^{-1}, first-order dependence on oxygen, and near inverse first-order dependence on carbon monoxide in good agreement with other flow system work such as that of Baddour *et al.* (*23*) and the references they quote. The same pattern prevails with iridium and rhodium and probably ruthenium although the results with the latter are complicated by time-dependent effects.

On the other hand, our results for platinum show a much lower activation energy and only a slight negative-order dependence on carbon monoxide. Recently there have been several other flow reactor studies of this system (*14*, *24*, *25*) each incorporating substantial water in the feed, and Table 6 compares their findings with our own. The agreement is reasonable for kinetic orders, but activation energies show a wide spread possibly reflecting support effects. These three earlier studies each found that results could be approximately described by Langmuir–Hinshelwood models based on relatively weak adsorption of *molecular* oxygen in competition with strongly adsorbed carbon monoxide. However, there seems to be no evidence at the molecular level for this model, whereas for reaction on better defined surfaces at lower pressures considerable direct evidence in favor of three other schemes does exist. It is therefore of interest to examine the extent to which these schemes might explain flow system results. The best documented steps for CO_2 production are: (i) an Eley–Rideal reaction between adsorbed oxygen atoms and gas phase CO (*2–4*, *6*, *12*),

$$\mathrm{O(a)} + \mathrm{CO(g)} \rightarrow \mathrm{CO_2(g)}; \qquad (1)$$

(ii) reaction between molecular oxygen physically adsorbed on *top* of a layer of adsorbed carbon monoxide,

$$2\mathrm{CO(a)} + \mathrm{O_2(a)} \rightarrow 2\mathrm{CO_2(g)} \qquad (2)$$

[the reaction was reported to be second order in adsorbed carbon monoxide (*12*)]; and (iii) a Langmuir–Hinshelwood reaction between oxygen *atoms* and adsorbed carbon monoxide (*2*, *3*, *6*),

$$\mathrm{CO(a)} + \mathrm{O(a)} \rightarrow \mathrm{CO_2(g)}. \qquad (3)$$

The steady-state equations for simultaneous occurrence of these three reactions on unit area of surface are then:

$$\begin{aligned} d\mathrm{O_a}/dt = {} & 2\sigma_{\mathrm{O_2}} Z_{\mathrm{O_2}} \theta_{\mathrm{u}} \\ & - n_{\mathrm{s}} \nu_{\mathrm{O}} \theta_{\mathrm{O}} \exp(-q_{\mathrm{O}}/RT) \\ & - \gamma Z_{\mathrm{CO}} \theta_{\mathrm{O}} \exp(-E_1/RT) \\ & - k_3 n_{\mathrm{s}}^2 \theta_{\mathrm{O}} \theta_{\mathrm{CO}} \exp(-E_3/RT) = 0 \end{aligned} \qquad (4)$$

TABLE 6

Comparison of Kinetic Parameters for Carbon Monoxide Oxidation over Platinum

Reference	Catalyst	Order in O_2	Order in CO	Activation energy (kJ mol^{-1})
(*14*)	Pt/Al_2O_3	1.0	−0.5[a]	87[a]
(*24*)	Pt/monolith	1.0	−0.5	67
(*25*)	Pt/fiberglass	1.07	−0.28	27
This work	Pt/SiO_2	0.9	−0.2	56

[a] Estimated for approximately 450 K from reported parameters for equation used to fit data.

and

$$dCO_a/dt = \sigma_{CO}Z_{CO}\theta_u - n_s\nu_{CO}\theta_{CO}\exp(-q_{CO}/RT) - 2k_2O_2(a)n_s^2\theta_{CO}^2\exp(-E_2/RT) - k_3n_s^2\theta_O\theta_{CO}\exp(-E_3/RT) = 0, \quad (5)$$

where the first term represents adsorption of reactants on unoccupied sites, θ_u, the second term desorption from occupied sites [nil in the case of oxygen atoms (*26*)], the third term CO_2 production via reactions (1) and (2), respectively, and the final term CO_2 production via (3). The other symbols are as defined in Table 7. While the model is far too crude to warrant exact use, we can employ it to predict conditions under which particular mechanisms are likely to control the rate of CO_2 production. If the values given in Table 7 for the various parameters are assumed the following regions may be identified for the pressures we employed.

TABLE 7

Parameters used in Equations (4) to (10)

Symbol and identification	Value	Reference
Z_{CO} [collision frequency for CO]		
Z_{O_2} [collision frequency for O_2]		
n_s [number of sites per unit area]	6×10^{18} m^{-2}	(*12*)
a_m [average area per surface atom]	8.4×10^{-20} m^2	
ν_{CO} [frequency of Pt–CO bond]	1.5×10^{13} s^{-1}	
q_{CO} [heat of adsorption of CO]	117 kJ mol^{-1}	(*5*)
σ_{CO} [sticking probability for CO]	0.6	(*4*)
σ_{O_2} [sticking probability for O_2]	0.1	(*4*)
γ [reaction probability for (1)]	0.13	(*4*)
E_1 [activation energy for (1)]	0.0 kJ mol^{-1}	(*12*)
E_2 [activation energy for (2)]	40 kJ mol^{-1}	(*12*)
E_3 [activation energy for (3)]	120 kJ mol^{-1}	(*6*)
k_3 [rate constant for (3)]	—[a]	—[a]
k_2 [rate constant for (2)]	—[b]	—[b]
O_2 [concentration physically adsorbed oxygen]	—[b]	—[b]

[a] From data in Ref. (*6*) we calculate that the term $k_3n_s^2a_m \times \exp(-E_3/RT)$ required to calculate (e) of Fig. 5 has the value $2.63 \times 10^{12}\exp(-14{,}469/RT)$.

[b] From the initial slope of Fig. 5 of Ref. (*12*) we estimate that $2k_2n_s^2a_mO_2$ (a) $\exp(-E_2/RT)$ [Eq. (6)] is given by 95 $(P_{O_2}/N\ \mathrm{m}^{-2})^{0.8}\exp(-4831/T)$.

Region I

At temperatures below 430 K the surface is almost entirely covered by CO, and the dominant reaction is (2). The equation for turnover number (rate per surface Pt atom of average area, a_m) is then,

$$\text{Turnover number} = 2k_2n_s^2a_mO_2(a)\exp(-E_2/RT). \quad (6)$$

From the results of Heyne and Tompkins (*12*) with no CO gas present one expects an activation energy of 40 kJ mol^{-1}, approximately first-order dependence on O_2, and probably near zero or slightly negative-order dependence in CO assuming only slight competition between O_2 and CO in second-layer adsorption. Our results at the lower temperatures conform to this picture.

Region II

At temperatures around 500 K the surface is still nearly covered by CO, but reaction (1) now dominates. However, CO desorption limits the turnover number which is given by,

$$\text{Turnover number} = (2\sigma_{O_2}Z_{O_2}n_sa_m\nu_{CO}/\sigma_{CO}Z_{CO}) \times \exp(-q_{CO}/RT). \quad (7)$$

Thus the reaction should be first order in O_2, and inverse first order in CO with activation energy equal to the heat of desorption of CO. The conditions of Langmuir (*1*) correspond to this situation, and ours may tend toward them at the highest temperature.

Region III

At still higher temperatures reaction (1) still dominates, but its rate becomes limited by the probability of reaction per collision and the turnover number expression is,

$$\text{Turnover number} = 2\sigma_{O_2}Z_{O_2}\gamma Z_{CO}a_m/(2\sigma_{O_2}Z_{O_2} + \gamma Z_{CO}). \quad (8)$$

The kinetics would be first order in CO and zero order in O_2 if $2\sigma_{O_2}Z_{O_2} \gg \gamma Z_{CO}$ and vice-versa if $\gamma Z_{CO} \gg 2\sigma_{O_2}Z_{O_2}$.

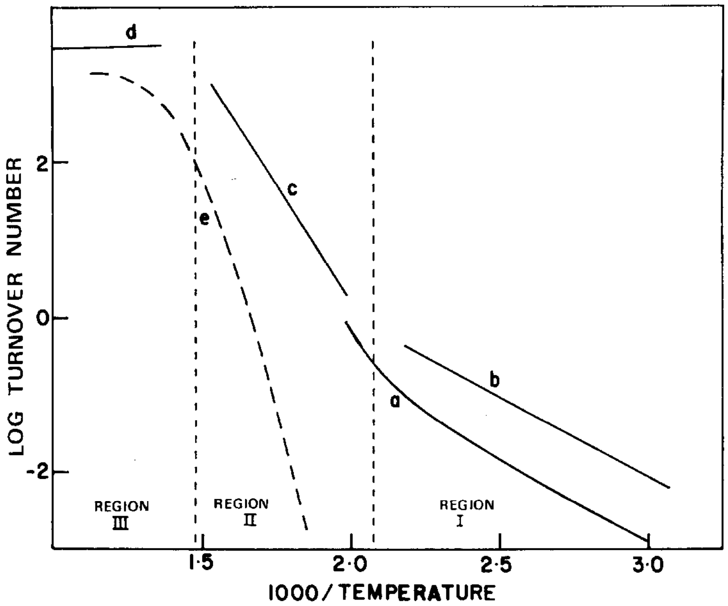

FIG. 5. Comparison of experimental and calculated temperature dependence for reaction over platinum with CO and O_2 pressures of 1300 and 650 $N\ m^{-2}$, respectively; (a) experimental; (b) Eq. (6) = $16{,}907 \exp(-4831/T)$; (c) Eq. (7) = $1.34 \times 10^{12} \exp(-14{,}092/T)$; (d) Eq. (8) $= 89{,}000/(T)^{\frac{1}{2}}$; (e) estimated for Langmuir–Hinshelwood reaction (3).

Figure 5 compares the temperature dependences predicted by equations (6), (7), and (8) with our experimental ones. Given that the basic parameters correspond to a very different conditions the similarity at the lower temperatures is sufficient to suggest that the major reaction under such flow conditions is identical to that observed by Heyne and Tompkins (*12*) in their experiments when CO gas was absent. Figure 5 predicts a transition to region II [where the Eley–Rideal reaction (1) controls] at the upper end of our experimental measurements, a trend with which the sparse data may conform. In regions II and III the Langmuir–Hinshelwood reaction of atomic oxygen (3) also takes place, but its calculated rate, plotted as (e) in Fig. 5, is always much less than that of the dominant process.

The foregoing model predicts changes in the kinetic order in carbon monoxide and/or oxygen during transition from region I to II or II to III. McCarthy *et al.* (*16*) reported such a change when oxidizing low pressures of CO with pure O_2, conditions which have the effect of bringing the intersection points between b, c, and d in Fig. 5 close together at their reaction temperatures.

At the interface between region II and region III the appropriate equation is

$$\text{Turnover number} = \frac{2\sigma_{O_2} Z_{O_2} \gamma Z_{CO} n_s a_m \nu_{CO} \exp(-q_{CO}/RT)}{\sigma_{CO} \gamma Z^2_{CO} + n_s \nu_{CO} (2\sigma_{O_2} Z_{O_2} + \sigma_{CO} Z_{CO}) \exp(-q_{CO}/RT)}, \quad (9)$$

while between region I and region II the full equation is

$$\begin{aligned}\text{Turnover number} &= 2k_2 n_s{}^2 a_m \theta_{CO}{}^2 O_2(a) \\ &\times (1 + 2\sigma_{O_2} Z_{O_2}/\sigma_{CO} Z_{CO}) \\ &\times \exp(-E_2/RT). \quad (10)\end{aligned}$$

Figure 6 shows log–log plots for the predictions of these two equations in comparison to the results of McCarthy *et al.* (*16*) for 1000-Å particles at 463 K. The parameters used are as given in Table 7 except that in the case of (10) we have extrapolated from our own experimental values assuming that $O_2(a)$ is now 0.5 order in oxygen (*12*) because of the high pressures of oxygen being used.

Both equations show rate maxima not too far from the experimental ones, but the turnover numbers in the first-order region are higher by more than an order of magnitude. On our model such a discrepancy can only be attributed to a value of γ [the reaction probability per collision for $O(a) + CO(g)$] much below the value of 0.13 assumed from uhv data (*4*). (This may be seen intuitively since, as pointed out by McCarthy *et al.* (*16*), the surface will be covered by oxygen in the first-order region, and thus the rate is controlled solely by the reaction rate between this adsorbed oxygen and gas-phase carbon monoxide.) The values of γ required to fit the results of McCarthy *et al.* (*16*) are about 0.0015, 0.00038, and 0.00012 for 1000-, 78-, and 28-Å particles, respectively.

If the values of γ were this small then the Langmuir–Hinshelwood reaction (3) could make a larger contribution in regions II and III than indicated by Fig. 5. Indeed for $\gamma = 0.0015$, the rate of CO_2 production via (3) is predicted to exceed that via (1) above about 680 K.

Other Noble Metals

The kinetic parameters we find for reaction over the other four metals are so different to those for platinum as to indicate a different mechanism. Indeed the activation energies and pressure dependences are consistent with the region II situation of Fig. 5 for which the controlling equation is (7):

$$\text{Turnover number} = (2\sigma_{O_2}Z_{O_2}n_s a_m \nu_{CO}/\sigma_{CO}Z_{CO}) \times \exp(-q_{CO}/RT).$$

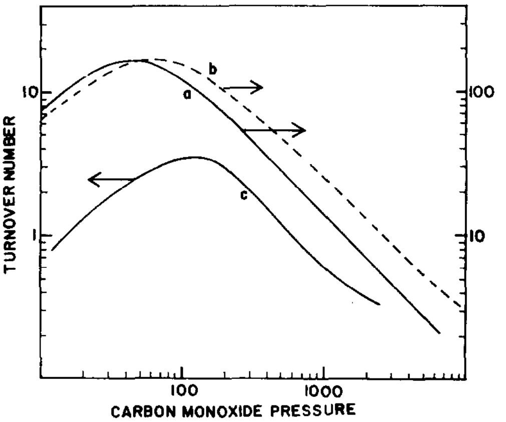

FIG. 6. Illustrative comparison of expected and observed dependence of reaction rate over platinum on carbon monoxide pressure at 463 K with oxygen pressure of 101 kN m^{-2}; (a) Eq. (9); (b) Eq. (10) with $2k_2n_s^2a_mO_2(a)\exp(-E_2/RT) = 0.76$; (c) experimental data as calculated from Fig. 3 of Ref. (*16*).

If our highest temperature measurements for platinum also conformed to that situation, as seems possible, then the order of activity for the five metals under these conditions should be primarily determined by the heat of adsorption of CO if the ratio $2\sigma_{O_2}Z_{O_2}/\sigma_{CO}Z_{CO}$ was similar for each metal. Accurate heats of CO adsorption for supported metals are not available so the best that can be done is to use heats of adsorption for a set of equivalent surface structures. The most complete tabulation appears to be that of Weinberg *et al.* (*7*) for the hexagonally close-packed planes. Their values are reproduced in the final column of Table 4.

Assuming those values we have used Eq. (7) to calculate the turnover numbers shown in the second last column of Table 4. The order in activity and the spread in relative activities correspond relatively well to the experimental ones although turnover numbers are two orders of magnitude low. It would require a lowering of about 18 kJ mol^{-1} in the assumed values for the heats of adsorption for closest agreement. Such a change is not unreasonable given the small dimensions of the supported metal particles and indeed more in line with the observed activation energies

(Table 1) with which the heats of adsorption should be equated in region II. Since the activity order of noble metals for the methanation reaction (*20*) (CO/H_2) is the same as for CO oxidation it is conceivable that it too is limited by the rate of CO desorption.

ACKNOWLEDGMENTS

Acknowledgment is made to the donors of the Petroleum Research Fund, administered by the American Chemical Society, for supporting this research. The Australian Research Grants Committee provided funds for purchase of some of the equipment used. Some of the initial and final experiments were carried out by Mr. D. J. Mackenzie and Mr. J. Kilford, respectively.

REFERENCES

1. Langmuir, I., *Trans. Faraday Soc.* **17,** 621 (1922).

2. Bonzel, H. P., and Ku, R., *J. Vacuum Sci. Technol.* 9, 663 (1972); *Surface Sci.* **33,** 91 (1972).

3. Winterbottom, W. L., *Surface Sci.* **36,** 205 (1973).

4. Nishiyama, Y., and Wise, H., *J. Catal.* **32,** 50 (1974).

5. Comrie, C. M., and Lambert, R. M., *J. Chem. Soc. Faraday Trans. I* **72,** 1659 (1976).

6. Pacia, N., Cassuto, A., Pentenero, A., and Weber, B., *J. Catal.* **41,** 455 (1976).

7. Weinberg, W. H., Comrie, C. M., and Lambert, R. M., *J. Catal.* **41,** 489 (1976).

8. Ertl, G., and Rau, P., *Surface Sci.* **15,** 443 (1969).

9. Ertl, G., and Koch, J. *in* "Adsorption–Desorption Phenomena" (F. Ricca, Ed.), p. 345. Academic Press, New York, 1972.

10. Close, J. S., and White, J. M., *J. Catal.* **36,** 185 (1975).

11. Kuppers, J., and Plagge, A., *J. Vacuum Sci. Technol.* **13,** 259 (1976).

12. Heyne, H., and Tompkins, F. C., *Proc. Roy. Soc. London Ser. A* **292,** 460 (1966).

13. Palazov, A., Chang, C. C., and Kokes, R. J., *J. Catal.* **36,** 338 (1975).

14. Voltz, S. E., Morgan, C. R., Liederman, D., and Jacobs, S. M., *Ind. Eng. Chem. Prod. Res. Develop.* **12,** 294 (1973).

15. Wei, J., *Advan. Catal.* **26,** 57 (1975).

16. McCarthy, E., Zahradnik, J., Kuczynski, G. C., and Carberry, J. J., *J. Catal.* **39,** 29 (1975).

17. Sinfelt, J. H., and Yates, D. J. C., *J. Catal.* **8,** 82 (1967).

18. Escard, J., Leclere, C. and Contour, J. P., *J. Catal.* **29,** 31 (1973).

19. Tauster, S. J., and Murrell, L. L., *J. Catal.* **41,** 192 (1976).

20. Vannice, M. A., *J. Catal.* **37,** 449 (1975).

21. Cant, N. W., and Hall, W. K., *J. Catal.* **16,** 220 (1970).

22. Ludlum, K. H., and Eischens, R. P., *Surface Sci.* **40,** 397 (1973).

23. Baddour, R. F., Modell, M., and Heusser, U. K., *J. Phys. Chem.* **72,** 3621 (1968).

24. Shishu, R. C., and Kowalczyk, L. S., *Platinum Metals Rev.* **18,** 58 (1974).

25. Nicholas, D. M., and Shah, Y. T., *Ind. Eng. Chem. Prod. Res. Develop.* **15,** 35 (1976).

26. Vanselow, R., and Schmidt, W. A., *Z. Naturforsch.* **22a,** 717 (1967).